Proceedings for the 2016 EUMETSAT Meteorological Satellite Conference, 26-30 September 2016, Darmstadt, Germany

A FUNDAMENTAL CLIMATE DATA RECORD THAT ACCOUNTS FOR METEOSAT FIRST GENERATION VISIBLE BAND SPECTRAL RESPONSE

F. Rüthrich[1], V. John[1], R. Roebeling[1], S. Wagner[1], B. Viticchie[1], T. Hewison[1], Y. Govaerts[2], R. Quast[3], R. Giering[3], J. Schulz[1]

[1]EUMETSAT, Darmstadt
[2]Rayference, Brussels, Belgium
[3]FastOpt,Hamburg,Germany

Abstract

The series of Meteosat First Generation (MFG) Satellites provides a unique opportunity for the monitoring of climate variability and possible climate change. Since the eighties, seven satellites were operationally employed; all equipped with similar MVIRI radiometers. The time series of available data now covers, for some parts of the globe, more than 34 years with a 30 minutes repeat cycle and sampling distance of 2.5 x 2.5 km² at the sub-satellite point for the visible band. Up till now, the lack of characterization of subtle differences between the radiometers in terms of the silicon photodiodes, the optical path, the degradation pattern and the variability due to other sources of uncertainties have limited the exploitation of this unique time series as a Fundamental Climate Data record (FCDR). With the EU Horizon 2020 FIDUCEO project (FIDelity and Uncertainty in Climate data records from Earth Observations) a European effort has been launched in order to re-calibrate and reprocess this time series and to provide its data as FCDRs, from which geophysical parameters, in particular Essential Climate Variables, can be derived. The FIDUCEO approach builds up on the calibration methodologies developed by the Global Space-based Inter-Calibration System (GSICS). Overall, the aims are the recovery of the MVIRI/VIS band sensor spectral response function (SSR), the enhancement of the calibration accuracy by accounting for the found SSR degradation, the application of a consistent calibration methodology over the entire time series, and the propagation of the measurement uncertainties to the FCDR according to metrological standards. While the recovery of the sensor spectral response is presented in detail in another contribution to this conference, this presentation has its focus on the integration of the recovered, temporally varying SSR to the generation of Meteosat/MVIRI radiances and on the accuracy of the enhanced FCDR.

INTRODUCTION

Meteosat First Generation (MFG) Satellites have been in Orbit since 1977. From 1981 on a rather consistent record of the retrieved imagery is available. The satellites were operated at two locations. The primary location at 0° longitude provides coverage over Europe and Africa. Overlapping with this primary coverage, some satellites were also used to provide Indian Ocean Data Coverage (IODC).

All MFG satellites employed similar Radiometers, the Meteosat Visible Infra-Red Imager (MVIRI), providing a high potential for consistency even when looking at very old observations. With its 22 years coverage at 0° (+IODC: 18y), this dataset provides indispensable data for periods where more precise technologies where not yet available. Revised calibration activities based on matchups with other sensors were carried out already for the Infrared channels of MVIRI. Examples are the Global Space-based Inter-Calibration System (GSICS: http://gsics.wmo.int/) or the strategy presented by Roebeling et al. (2013). However, a consistent revision and -calibration of the MVIRI VIS band has not yet been provided.

The presented work is carried out in the course of the project “Fidelity and uncertainty in climate data records from Earth Observations” (FIDUCEO). It aims on putting this dataset as a fundamental climate data record (FCDR) into value for climate studies, for atmospheric reanalysis and for level 2 retrievals. It involves the

completion of the uncertainty budged, correction of noise estimations, recalibration activities and the recovery of spectral degradation of the sensor responsivity.

MEASUREMENT SETUP

MFG are spin stabilized geostationary satellites, operated at an altitude of around 35000 km. During each revolution of the satellite the MVIRI radiometer uses it's two operational silicon detectors to acquire two scanlines. This way, with a spin rate of around 100 rpm, the entire face of the earth is sampled within 25 minutes into 5000 scan lines, each containing 5000 pixel. The signal obtained from the detectors is converted into a digital 8 bit signal (6 bit for the early satellites until MET3) and sent to earth.

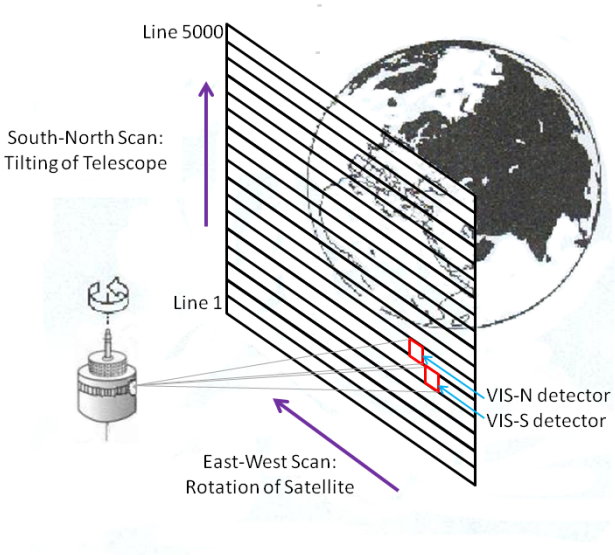

***Figure 1*: Sketch of the measurement setup for Meteosat First Generation satellites**

MEASUREMENT EQUATION

The unit of the FCDR will be that of Bidirectional Reflectance Factor (BRF) (Nicodemus et al., 1977). Given the signal being sent to earth as a unit less digital count, this requires calibration and conversion. The measurement equation for this purpose is given in Equation 1,

$$\rho(xyt) = \frac{(K_E(xyt) - K_S(t))(a_0 + a_1 D(t))}{cos(\theta(xyt))} \frac{\pi d^2}{\int_\lambda \xi(t\lambda) I(\lambda) \Delta\lambda} \quad \textbf{(1)}$$

with the terms being:

ρ	BRF
x	pixel number (location in x direction)
y	line number (location in y direction)
t	time
K_E	Earth-count
K_S	Space-count
a_0	calibration coefficient at launch time
a_1	calibration coefficient time dependency
D	days since launch
d	sun-earth distance

θ solar zenith angle
λ wavelength
I solar spectral irradiance
ξ spectral response function

The two parameters related to the calibration, a_0 and a_1, are determined using vicarious calibration. For this purpose radiative transfer modelling is performed above pseudo-invariant calibration sited of two types: Sea and desert (Govaerts et al. 2004).

EFFECTS CAUSING UNCERTAINTY

Every term in the measurement equation is subject of effects that are causing uncertainty, which is propagated according to metrological standards into the combined standard uncertainty of the reflectance. Correlations of the uncertainties in space or time are explicitly considered. In Table 1 a summary of the considered effects is presented.

***Table 1*: Overview of the uncertainty effects that are foreseen to be considered in the FCDR**

1	Digitization noise
2	Earth count noise
3	Space count noise
4	Photonic noise
5	Location uncertainty (latitudinal)
6	Location uncertainty (longitudinal)
7	Acquisition time uncertainty
8	SZA uncertainty
9	Sensor drift uncertainty
10	Uncertainty of gain at launch
11	Spectral response uncertainty
12	Solar Irradiation uncertainty
13	Earth-sun distance uncertainty

Note that not all of those effects directly influence the uncertainty in the measurement equation. This is e.g. the case for the acquisition time uncertainty. The acquisition time uncertainty determines - together with the longitudinal location uncertainty - the uncertainty of the local hour angle at a pixel location. Only mediated through this, it feeds into the uncertainty of the solar zenith angle which then is part of the measurement equation.

Note furthermore that one effect can also influence multiple terms of the measurement equation. This is e.g. the case for the location uncertainty. Location uncertainty, as mentioned above, may feed into the uncertainty of the solar zenith angle. However, it may also affect the uncertainty of the count value measured at a given location. The sensitivity of this is of course depending on the spatial count gradients that are present at that location.

EXAMPLE 1: EARTH COUNT NOISE

A usual measure to determine the radiometric noise which is present in geostationary satellite data is the combined standard deviation in the space corners of an image. This is based on the assumption that the signal received from space is zero and that all variability must be caused by the noise of the different electronic elements of radiometer and satellite. To sample this varability appropriately, the radiometers from MET4 onwards were designed to add an offset of 100 mV to the signal.

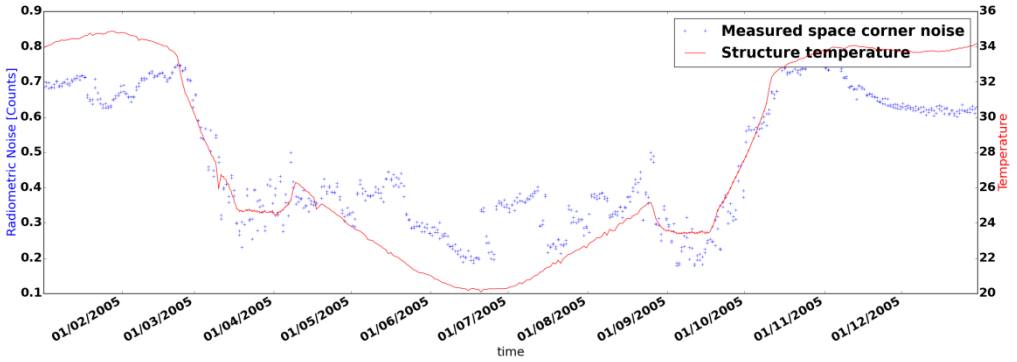

***Figure 2*: Time series of Meteosat 7 space corner noise of one of the two visible detectors plotted with interior temperature during 2005 noon slots. The temperature is particularly that of the structure where the analog-digital converter is mounted.**

For the space corner standard deviations we observe a close co variation with the temperature inside the satellite (Figure 2). For the detection chain of visible sensor VIS1 it is possible to explain around 90% of this variability only by considering the structure temperature and the temperature dependency of the analogue-to-digital (A/D) converter. This temperature dependency was characterized in pre-flight measurements, where the voltage levels at the A/D converter switches were shown to decrease with temperature. With this, the space corner standard deviation may not fully represent the noise level of earth counts, because this latter is independent from the A/D converter switches.
In order to obtain a more appropriate estimate of the earth count noise an inverse method is developed to determine the parameters of a simple earth count noise model of the form:

$$\delta_R K_1(t) = \frac{\sigma N_0 + F_T * (T(t) - T_0)}{\Delta S} \qquad \textbf{(2)}$$

where:

$\delta_R K_1$	Earth count noise of detector VIS1
σN_0	Standard deviation of the sensor voltage which is fed into the A/D converter at T_0
F_T	Factor by which standard dev. of sensor voltage increases with temperature
T	actual temperature of mounting structure on spacecraft
T_0	reference temperature (minimum temperature of structure)
ΔS	step-with of A/D converter in mV

As depicted in Figure 3, the magnitude and time variance of the modelled noise series underlines the expected difference from that of the space corner noise.

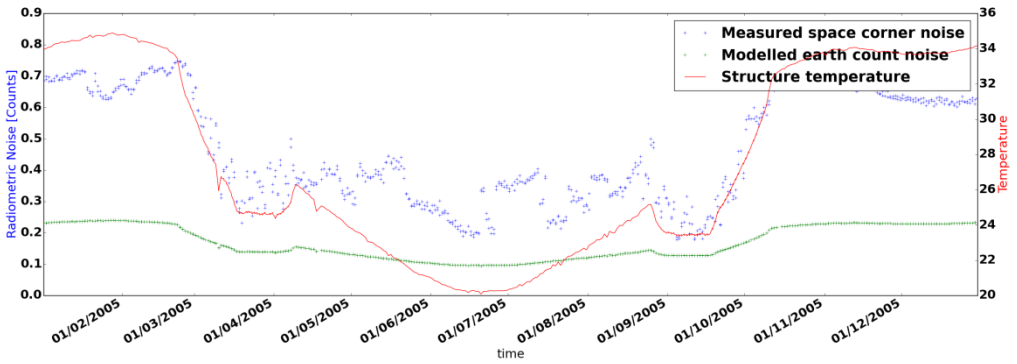

***Figure 3*: Time series of Meteosat 7 modelled earth count noise for VIS1 detection chain, overlaid with the measured space corner noise and with the interior temperature during 2005 noon slots. The temperature is particularly that of the structure where the analog-digital converter is mounted.**

This is then combined with photonic noise and digitisation noise as the root of sum of squares and used for propagation into the combined standard uncertainty of the earth count.

EXAMPLE 2: SENSOR SPECTRAL RESPONSE

The uncertainty of the spectral response function affects also the uncertainty of the calibration parameters a0 and a1. Unfortunately, the pre-flight characterizations of the SSR, particularly for the older satellites, are problematic (Decoster et al 2013, Govaerts 1999). To make things worse also spectral degradation was observed (e.g. Decoster et al 2014). Spectral degradation in this case means the time dependency of the calibration coefficients, aka drift or degradation, is faster in the blue parts of the spectrum than in the red. This is illustrated in Figure 4 where the drift rate above sea targets with their rather bluish spectrum is greater than above the desert targets.

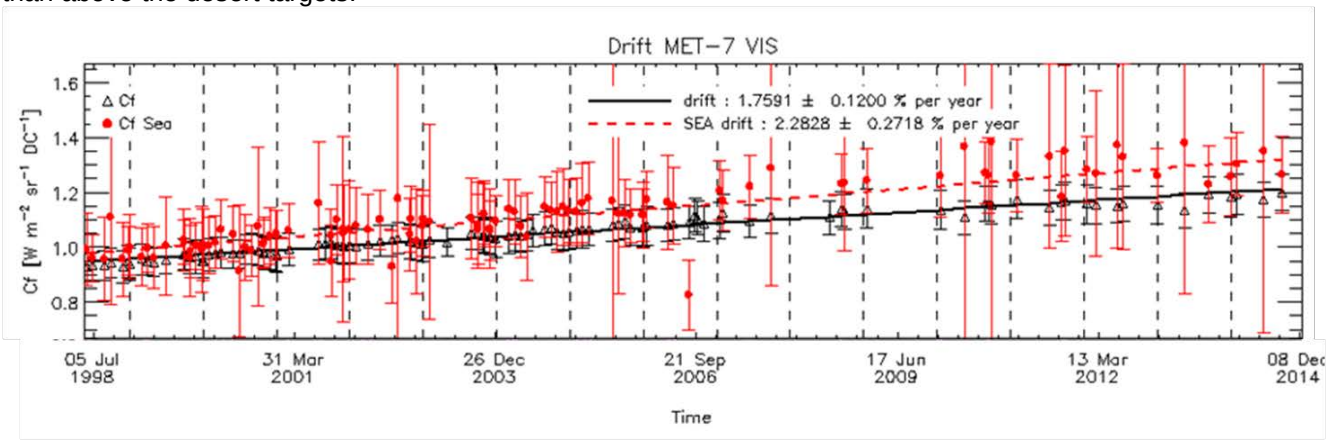

***Figure 4*: Calibration coefficients obtained within the lifetime of Meteosat 7 above two different target types (black: desert; red: sea).**

Such an effect is problematic for an FCDR because the correct estimation of the uncertainty of a measured reflectance value would always require a priori knowledge about the underlying spectrum.
One major innovation of the presented FCDR venture is the development of a reverse engineering methodology for the in-flight determination of the spectral response function and for the monitoring of its spectral degradation. This methodology is presented in Govaerts et al (2016).
The corrected spectral response functions are then fed into the calibration process to correct for the related effects and to determine the remaining uncertainties properly.

EXAMPLE 3: SZA UNCERTAINTY

The solar zenith angle uncertainty in the presented FCDR can be traced back to the uncertainties of the location of each pixel (Figure 5) and to the uncertainty of its acquisition time (Figure 6).

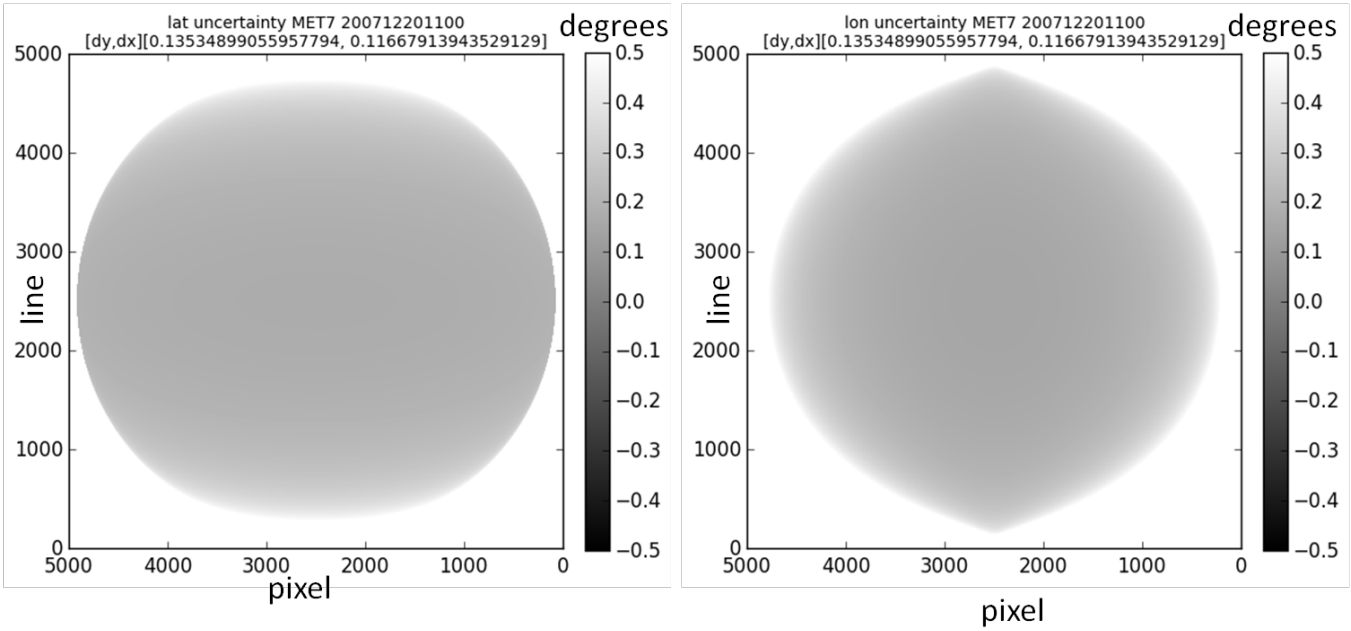

***Figure 5*: Example for the pattern of longitudinal and latitudinal location uncertainties in an example image of Meteosat 7.**

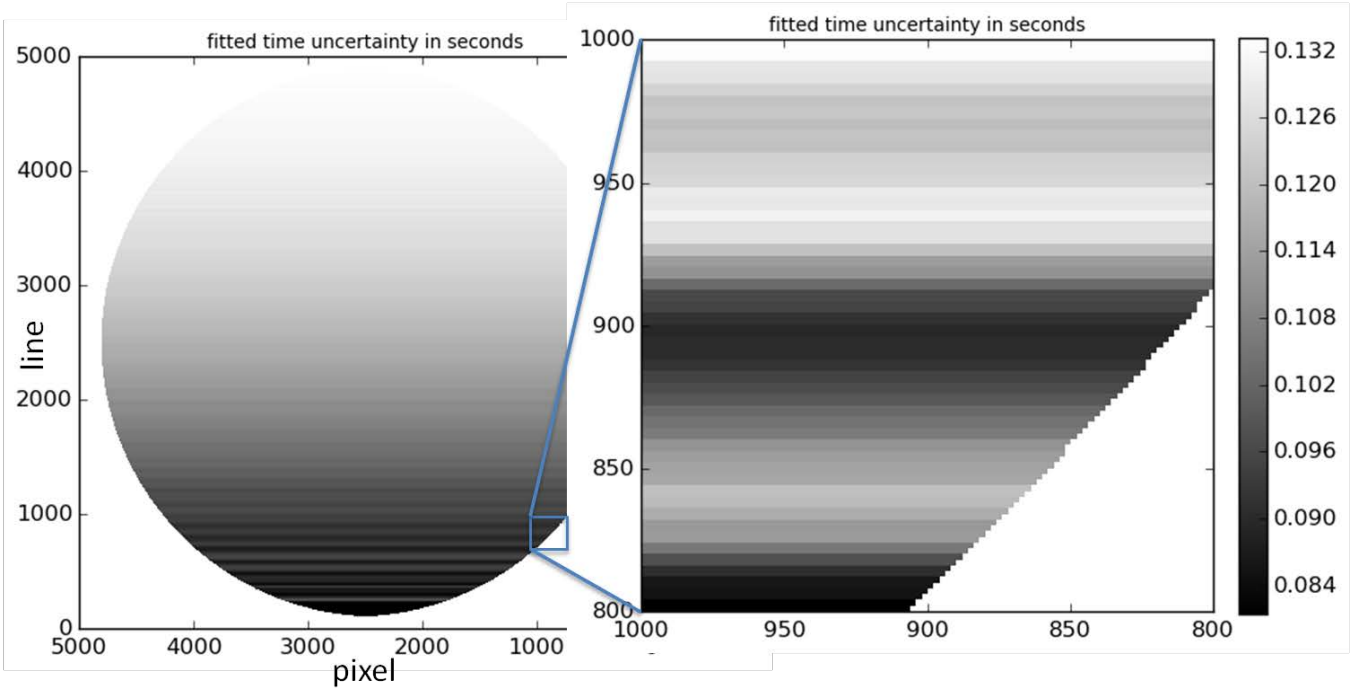

***Figure 6*: Example for the pattern of acquisition time uncertainties in an example image of Meteosat 7.**

Particularly the location uncertainties are strongly correlated. Correlation coefficients for the example image acquired in December 2007 are given in Table 2.

***Table 2*: Correlation coefficients for the uncertainties that contribute to the solar zenith angle uncertainty**

	δtime	δlat	δlon
δtime	1	~0	~0
δlat	~0	1	≈0.7
δlon	~0	≈0.7	1

The framework used for the propagation considers the covariance according to the Guide to the Expression of Uncertainty in Measurement (GUM; JGCM 2008). It will be published separately in the course for the Fiduceo project (http://www.fiduceo.eu/).

OUTLOOK

The MVIRI VIS FCDR is intended to be used for the creation of level 2 datasets on albedo and aerosol. Therefore a joint Albedo/Aerosol retrieval is developed and will be applied on both, the new FCDR and on the data with the currently available calibration. This will help to characterize and validate the impact of the new methodology for tracing uncertainties and recovering the SSR.

Apart from this the intense revision of the dataset in the course of the presented activity also initialized further amendments of the dataset. A good example is the evaluation of the expectations from a methodology that calibrates each individual detector separately.

ACKNOWLEDGEMENTS

FIDUCEO has received funding from the European Union's Horizon 2020 Programme for Research and Innovation, under Grant Agreement no. 638822.

REFERENCES

Decoster I., Clerbaux N., Govaerts Y. M., Baudrez E.,Ipe A., Dewitte S., Nevens S. (2013). Evidence of pre-launch characterization problem of Meteosat-7 visible spectral response, Remote Sens. Lett**. 4(10)**, 1008-1017. doi:10.1080/2150704X.2013.828181

Decoster I., Clerbaux N., Baudrez E.,Ipe A., Dewitte S., Ipe, A., Nevens S., Velazquez Blazquez, A. And Cornelis, J. (2014). Spectral Aging Model Applied to Meteosat First Generation Visible Band Remote Sens. **6**, 2534-2571; doi:10.3390/rs6032534

Govaerts Y. (1999). Correction of the Meteosat-5 and -6 radiometer solar channel spectral response with the Meteosat-7 sensor spectral characteristics, Int. J. Remote Sens. **20(18)**, 3677-3682. doi:10.1080/0143 11699211273

Govaerts Y., Clerici M., Clerbaux N. (2004). Operationalcalibration of the Meteosat radiometer VISband, IEEE Trans. Geosci. Remote Sens. **42(9)**, 1900-1914. doi:10.1109/TGRS.2004.831882

Govaerts Y., Quast R., Ruethrich F., Giering R. And Roebeling R. (2016). Recovery of MVIRI/VIS Band Spectral Response. Proceedings for the 2016 EUMETSAT Meteorological Satellite Conference, 26-30 September 2016, Darmstadt, Germany

JCGM (2008). Evaluation of measurement data — Guide to the expression of uncertainty in measurement (GUM).

Nicodemus, F. E., J. C. Richmond, J. J. Hsia, I. W. Ginsberg, and T. Limperis. 1977. 'Geometrical Considerations and Nomenclature for Reflectance'. National Bureau of Standards.

Roebeling, R., J. Schulz, T. Hewison, and B. Theodore (2013). Inter-calibration of METEOSAT IR and WV channels using HIRS, AIP Conf. Proc. ,**288**, 288–291, doi:10.1063/1.4804763.